Metallurgical and Materials Engineering *Research paper*
Association of Metallurgical Engineers of Serbia AMES *https://doi.org/10.30544/495*

MICROSTRUCTURAL AND MECHANICAL BEHAVIOR OF Al 6061/SiC-Al_2O_3 COMPOSITES PROCESSED THROUGH FRICTION STIR PROCESSING

Ch. Mohana Rao [1], K. Meera Saheb [2]*

[1]Research Scholar, Dept. of Mechanical Engineering, JNTUK, Kakinada, AP, India
[2]Professor, Dept. of Mechanical Engineering, University College of Engineering Kakinada, JNTUK, Kakinada, E.G. Dist., AP, India, Pincode: 533003

Received 03.05.2020
Accepted 17.08.2020

Abstract

Metal Matrix Composite (MMC) reinforced in friction stir processing (FSP) has increased insights that can affectively attain the desired mechanical properties for the manufactured samples. The favorable conditions of carbides are considered for reinforcing the SiC particles into the Aluminum 6061. The methodology of fabricating Aluminum 6061 comprises of three materials, Al 6061-SiC-Al_2O_3. The experimental evaluation of the composite Aluminum 6061-SiC-Al_2O_3 includes the influence of process parameters on microhardness, tensile strength, and microstructure. As a result of the reinforcement of nanoparticles processed in FSP, the properties of composite material increased satisfactorily. The sample S3 observed to be having a maximum tensile strength of 185 MPa. The larger, the better condition is adopted to analyze the tensile strength of the fabricated samples. The optimum condition for maximum tensile strength was found at 900 RPM, 15 mm/min, and composition 3. The hardness profiles at different zones of friction stir processing (FSP), viz., Heat Affected Zone (HAZ), Thermo Mechanical Affected Zone (TMAZ), Nugget Zone (NZ) were examined. The characterization techniques deployed were optical microscope (OM), and scanning electron microscope (SEM) studies for microstructural behavior. The result shows that the reinforcements were tightly embedded into the base material surface. The spherical grains are formed in the reinforcement region.

Keywords: FSP; microhardness; tensile; OM; SEM; EDAX; taguchi; ANOVA.

*Corresponding author: Ch. Mohana Rao, *mohanarao23@gmail.com*

Introduction

The unique properties of aluminum and Al alloys laid a path for the researchers to enhance their properties through reinforcement. The applications which evolved in the automotive and aerospace industries [1–3] are the implications of their premium qualities such as high strength to weight ratio and low density. Al is used as the primary matrix material for most of the composite materials combination due to the high strength to weight ratio. The reinforced materials or Metal matrix composites (MMCs) are manufactured by a combination of specific materials with an appropriate ratio. Hence MMCs exhibit high-end qualities than alloys and its pure form of materials [6-7]. The bulk reinforcement may lead to change the entire properties of the base material. Hence fabrication or surface modification with nano-ceramic particles can be deployed to enhance the properties of the fabricated material without changing the unique mechanical properties of the base material [8-9].

The effective results of surface characteristics can be identified when high temperature is applied, rather than conventional surface treatments [10]. Hence surface fabrication is essential, and the operation should be under the melting point of the material to be fabricated for better and equal distribution of particles. The microstructure and strength of the base material will be modified [11] due to the fabricated composite, which is prepared by FSP. Solid-state welding is an appropriate method for welding dissimilar materials. Because for these practices, fusion is not necessitated, weld solidification outrageous does not occur. Solid-state processes resolve several other aluminum alloy fusion welding problems such as brittle inter-metallic shape, segregation, porosity, and liquidation cracking of the field. For welding of dissimilar materials, solid-state welding processes have got more attraction and appropriate for inducing different mutually exclusive configurations. Thanks to the possible technical significance and the difficulties associated with conventional welding, Friction Stir Welding of dissimilar alloys/metals has caught research interest. In the FSW process, small and approximately equal dimensions of recrystallized grains are shaped and established at high temperatures as the base material is subjected to extreme plastic deformation. The fine friction swirl welded microstructure provides strong mechanical properties. The metrics of the welding parameters, design of the joint, and tools are the important parameters that influence the pattern of sample movement and the spread of temperature, thus influencing the material's microstructural evolution.

The comprehensive list of parameters for the FSW process is outlined as:

i. Tool rotational speed (RPM).
ii. Welding speed or transverse speed (mm/min).
iii. Tool geometry.
    (a) Pin profile.
    (b) Tool shoulder diameter, D (mm).
    (c) Pin diameter, d (mm).
    (d) D/d ratio of the tool.
    (e) Pin length (mm).
    (f) Tool inclination angle (°).

Literature reveals those parameters' effects of mechanical and microstructure [12-13]. *Koilraj et al.* [14] used L16 Taguchi design to join dissimilar plates of Al–Cu alloy using friction stir process, and the observation reveals that tool shoulder diameter has a valid and weighted effect in determining the joint strength. Also, HAZ has low hardness among all processed regions. *Lakshminarayanan et al.* [15] observed the influence and effect of process parameters upon the weld strength of RDE Aluminum alloy using FSW. RDE 40 is a trading name of self-aging aluminum alloy in the Al-Zn-MG alloy family, having high strength and corrosion resistance. It has an ultimate tensile strength of 40 kg/sq. mm. These are mostly used for lightweight applications. Taguchi design was used for experimental analysis. It was observed that the axial force, welding speed, and rotational speed (RS), are the most influencing factors which impact tensile strength. The optimum tensile strength was observed to be 303 MPa. *Wang et al.* [16] used the Friction stir process (FSP) for surface modification of metallic materials with reinforcements of SiC particles in the Al matrix. There is good bonding strength, and the reinforcements are uniformly distributed. It was found that the microhardness of prepared surface composite is higher than the base material. Cavaliere [17] conducted experiments with 20% Al_2O_3 reinforcement in Al 2618 base material in Friction Stir Process (FSP). Intense temperature affected tensile tests were conducted to observe the rate of change in the strain at different temperatures. This mechanism is experimented at higher levels of temperature and varied strain rates in the NZ, to deduce the superplastic properties of the fabricated recrystallized material and to make out the variations with the higher hierarchy material which shows strong grain refinement because of Friction Stir Process. Elangovan [18] processed Al 6061 alloy by Magnesium and Silicon alloy with the FSW process to study the effect of different tool pin profiles (straight cylindrical, tapered cylindrical, threaded cylindrical, triangular and square) of joints. Among all the pin profiles and shoulder diameter, a square pin profile with an 18 mm shoulder has better performance. Elangovan [19] used the FSW process to join the Al 6061 alloy, and a mathematical model has been developed to estimate the tensile strength. *Rao. C.M. et al.* [20] experimented with TiB_2 and Aluminium composite, and wear studies were conducted on the reinforced material. Nascimento [21] compared FSP processed AA7072-T6 and AA5083-O with various tool geometries. Out of the two tool geometries, VFPS has better performance than SFSP. *R. S. Mishra et al.* [22] discussed Aluminum surface composites prepared by FSP with SiC particles. Samples are rotated and traversed with and without SiC powders at different tools. There has been evidence of increased rotational and traverse concentrations producing a more consistent distribution of SiC particles. The hardness of the developed composite surfaces was three times greater than that of the base material. The bending strength of the composite metal matrix was significantly greater than that of the polished plain specimen and raw base metal. The process of experiments after the FSP technique and characterization of composites [23] studied. *S Soleymani et al.* [24] explored microstructural and tribological properties of MoS_2 and SiC particles, reinforced with Al 5083 surface hybrid composite produced by FSP, as well as the dominant wear mechanisms operating under dry sliding conditions of the samples. The uniform distribution of reinforcing particles within the processing region and strong bonding between the surface processing layer and the base material was observed. The findings revealed that light delamination and light abrasion processes were worked concurrently when the hybrid composite was worn. It was found that the development of hybrid composite on the

surface considerably minimized wear damage and strengthened the alloy's wear resistance. Composites reinforced by SiC Particle Al matrix (SiC / Al) have drawn considerable interest from industry and scientists. For these, large volume fraction Al-matrix composites with SiC particle content usually ranging from 40 vol percent to 70 vol percent are mostly used because of their possibility of achieving an appropriate balance of desired properties like high modulus, low density, high thermal conductivity, low CTE, etc. [25]. The related work is carried out to deduce improving factors that affect the MMC. Base material Al 6061 is utilized in the experimentation. By adding calculated and varied amounts of SiC-Al_2O_3 to the Al 6061 alloy surface (the material is divided into nine equal parts), FSP is carried out and reinforced. As the literature on process optimization of Al 6061- SiC- Al_2O_3 fabrication is limited, this work focuses on finding out the optimized values of mechanical strength and exploring the microstructure at different phases of fusion zones during FSP.

Experimental approach

Aluminum 6061 material had been cut into plates of 150 mm X 37.5 mm X 6mm sized plates. The cut plates were taken, and grooves were shaped on the nine plates of Al 6061 with a scale of 1.5 mm width and 3 mm depth. H13 tool steel is considered for performing FSP. Fig.1 depicts the outline of the sequence of steps for the preparation of surface composites, followed by an interpretation of the executing implementation.

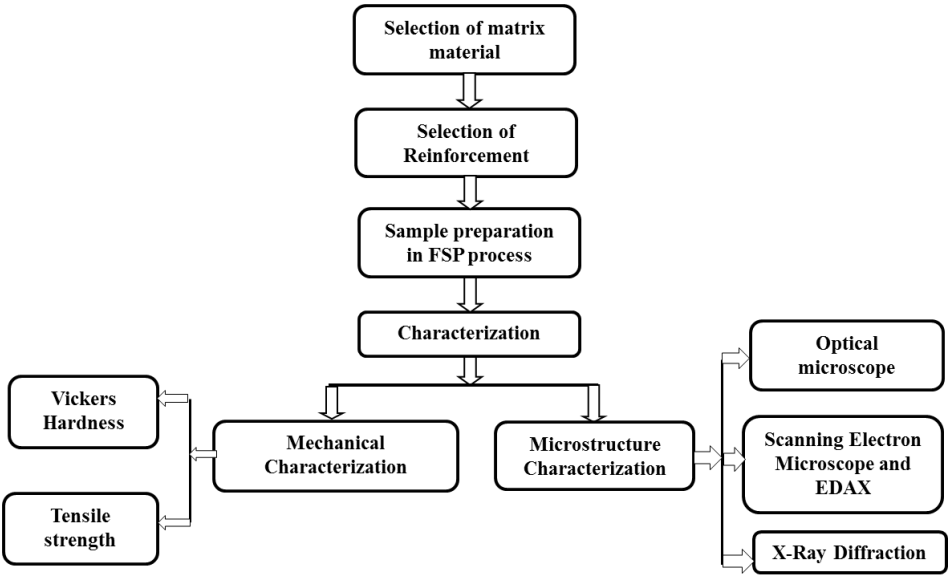

Fig. 1. Flow chart showing the sequence of steps involved in the process.

Preliminary arrangements of experimentation:

Choosing the base material, fabricating particles and tool

The chemical composition of Al 6061 is depicted in Table1. The surface alloying treatment is performed on 6.35 mm thickness plates, as explained in the previous section. The compositions are verified with the XRD technique, NIT Warangal, Telangana, India.

Table 1. Chemical composition of Al 6061-T6 Aluminum alloy (wt. %).

Element	Mg	Si	Cu	Zn	Ti	Mn	Cr	Al
Wt. %	0.85	0.68	0.22	0.07	0.05	0.32	0.06	Balance

The nanoparticles of SiC and Al_2O_3which measures 35 nm of size were taken as reinforcement particles for Al 6061 surface treatment. As the AISI H13 tool-steel gives the best results when hardened and tempered, the tool material used was subjected to hardening and tempering. Chemical materials of the AISI H13 tool steel are presented in Table2. The shoulder rod is cylindrical, measures 24 mm diameter; a taper surface diameter is 6mm at the end, and the pitch is 0.75 mm.

Table 2. Chemical composition of AISI H13 tool steel.

Element	C	Cr	Mo	V	Si	Mn	P	S	Fe
Wt. %	0.42	5.20	1.45	1.05	1.00	0.28	0.015	0.003	Balance

Experimentation and Optimization

Taguchi experimental design

Design of Experiments (DoE) was performed using the Taguchi methodology. The methodology investigates the effects of noise factors in the FSP. Parameter setting plays a vital role in the optimization of multiple characteristics. The L9 Taguchi design with parameters of three-levels and three-factor arrangement is selected for experimentation. The grooves with the dimensions of 3 mm depth and 1.5 mm width are filled with varied compositions of SiC and Al_2O_3 particles. The three compositions concerning the volume of the groove are:

a) *Composition 1*: 80% of SiC and 20% of Al_2O_3

b) *Composition 2*: 70% of SiC and 30% of Al_2O_3

c) *Composition 3*: 60% of SiC and 40% of Al_2O_3.

The FSP was performed on 'Friction Stir Welding -3T-NC' machine by varying the rotational speed (RS), travel speed (TS), and the above said compositions. The parameters set for the machine are *i) tilt angle of 2°, maintained constant,* and *ii) the axial load is 10KN.*

The L9 Taguchi factors are shown in Table3.

Table 3. L9 Experimental design for experimentation.

S. No	Rotation Speed (RPM)	Travel Speed (mm/min)	Weight/Volume % (SiC/ Al_2O_3)
1	900	15	Composition 1
2	900	25	Composition 2
3	900	35	Composition 3
4	1150	15	Composition 2
5	1150	25	Composition 3
6	1150	35	Composition 1
7	1400	15	Composition 3
8	1400	25	Composition 1
9	1400	35	Composition 2

Taguchi describes quality in two parts: quality management offline and online. There is a difference between conventional experimental design and Taguchi robust design. The conventional design aims at quality characteristics. Taguchi design focuses on minimizing the variance of the experimental results. The system, Parameter, and Tolerance are the influential design considerations in Taguchi.

The process parameter optimization for any experimentation was carried out through the below steps

Step 1: Determination of quality characteristic
Step 2: Categorize the test conditions and noise factors
Step 3: Recognize the factors which control and respective levels
Step 4: Experiment as per the design
Step 5: Data analysis
Step 6: Finding optimum process parameters

Selection of orthogonal array (OA)

Three parameters with three levels are considered for the current investigation. L9 Orthogonal Array is used for experimentation. Interaction effects are neglected for the study, and the main effects plots are considered into account for experimental design. For the present study, three parameters are selected, which have two degrees of freedom (DOF) for each factor; hence the total DOF would be 3*2 = 6. In general, the DOF of any experimental design is chosen in such a way that the total DOF of the factors is larger than the summation of DOF of all the factors. The possible standard orthogonal array that can be selected is L9 since it has 8 DOF; hence it is most suitable to estimate the main effects of the experimental study.

S/N calculation

The S/N ratio is intended on the qualitative characteristics of the response. There are three ways on which response characteristics are estimated and for the maximization problems: larger the better, in the case of minimization problems: smaller the better and nominal the better condition for general-purpose conditions. In the present scenario,

maximum tensile strength is desired for the processed joints, hence larger the better condition is followed.

$$S/N\ ratio(\eta) = -10\log_{10}\frac{1}{n}\sum_{i=1}^{n}\frac{1}{y_i^2} \qquad (1)$$

Wire cut and Specimen preparation

Fig.2. depicts the wire-cut performed on the FSP completed material. The processed FSW plates were subjected to EDM for wire-cut for tensile test, hardness, and other metallographic tests, where the fabricated area is considered in gauge length. To interpret the microstructural properties and know the presence of chemicals in terms of the composition of the FSP reinforced surface, SEM and EDAX are the methodologies used.

Fig. 2. Image of the Tensile Specimen Processed through EDM.

The identification and presence of different alloys in the surface reinforced sample at different phases are detected using X-ray diffraction (XRD), SEM notices the microstructure.

Measuring Micro-Hardness

The prerequisite of measuring hardness is removing the impurities on the fabricated surface. For removing impurities, the surfaces are cleaned with acetone. At the various zones of the reinforced surface, 50 g load will be applied for 15 sec of idle time. The hardness values at different zones to be collected.

Tensile Test

A total of nine tensile test specimens were collected from the wire-cut samples, which are cut using the EDM machine and followed the ASTM E8 standard, which is depicted in Fig.3. Universal Testing Machine, NIT, Warangal, Telangana State, was utilized for conducting the tensile test. The tests were conducted with different loads of

an electronic controller. The extracted (wire-cut) tensile test sample from the FSP plate is shown in Figure 2.

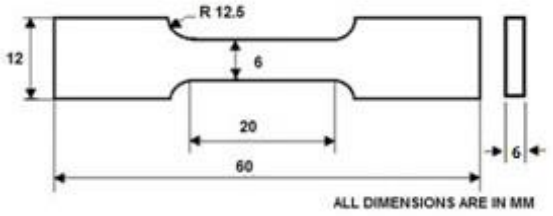

Fig. 3. Schematic design of specimen for the tensile test (as per ASTM).

Results and analysis

Taguchi analysis

Nine plates of Al 6061 with various compositions of SiC and Al_2O_3 are reinforced. After performing FSP, the samples were performed wire-cut with EDM Machine. The nine tensile specimens extracted from the fabricated plates through wire-cut (shown in Fig. 2) were tested with Ultimate Tensile testing Machine for their strength at the joints. The results obtained for nine tensile specimens are tabulated in the Table 4. As the Ultimate Tensile Strength (UTS) requires the maximum value for the better results, the 'larger the better' scenario is considered while calculating the S/N ratios in Taguchi design. The results are analyzed based on the previously said scenario.

The graph shown in Fig. 4 plots the main effects for means of tensile strength for the sample. The maximum tensile strength is observed at 900 RPM, 15 mm/min travel speed, and composition 3 (60-40), which is evident from Fig. 4. The fractography of these samples was also taken for further work.

Table 4. Response table for tensile strength of Al_2O_3 and SiC.

S. No	Rotation Speed (RPM)	Travel Speed (mm/min)	Weight Volume % (SiC/ Al_2O_3)	Ultimate Tensile Strength	S/N Ratio (Larger the better)
1	900	15	Composition 1	156.3	43.8792
2	900	25	Composition 2	165.0	44.3497
3	900	35	Composition 3	185.0	45.3434
4	1150	15	Composition 2	156.0	43.8625
5	1150	25	Composition 3	168.0	44.8241
6	1150	35	Composition 1	141.0	42.9844
7	1400	15	Composition 3	126.0	42.0074
8	1400	25	Composition 1	89.0	38.9878
9	1400	35	Composition 2	105.0	40.4238

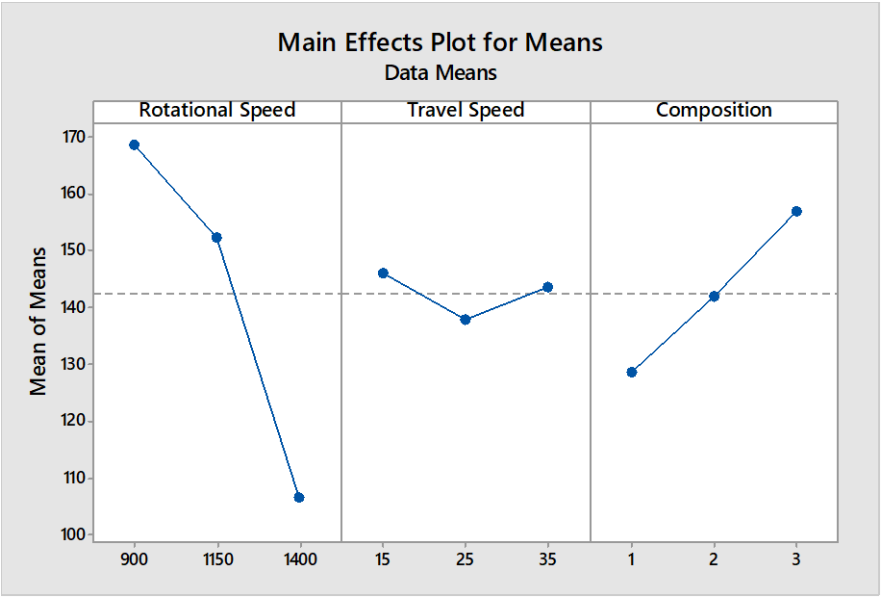

Fig. 4. Main effects plot for means.

Table 5. Response Table for Signal to Noise Ratios (the larger, the better).

Level	Rotational Speed	Travel Speed	Composition
1	44.52	43.25	41.95
2	43.64	42.47	42.88
3	40.47	42.92	43.81
Delta	4.05	0.78	1.86
Rank	1	3	2

Table 6. ANOVA for tensile strength.

Source	DF	Adj SS	Adj MS	F-Value	P-Value
Regression	3	6989.18	2329.73	21.37	0.003
Rotational Speed	1	5784.62	5784.62	53.05	0.001
Travel Speed	1	8.88	8.88	0.08	0.787
Composition	1	1195.68	1195.68	10.97	0.021
Error	5	545.19	109.04		
Total	8	7534.37			

The final equation of Ultimate Tensile Strength for regression model can be written as follows:

UTS (MPa) =
*260.2 - 0.1242*Rotational Speed - 0.122*Travel Speed + 14.12*Composition*

Table 5 explains the influential factor in the entire experimentation. The comparative analysis is performed, and ranks are assigned depending on the significance of the parameter. From Table 5, it is evident that the significance of the parameters follows the below order:

Rotational Speed > Composition > Travel Speed

The rotational speed is the most influential characteristic compared to Composition and TS. ANOVA is performed for ultimate tensile strength, shown in Table 6. The p-value< 0.05 for rotational speed and composition. Hence, the rotational speed and the later follow the above-mentioned order of significance in estimating and calculating the responses.

Tensile behavior due to the change in process parameters (Effects):

The tensile strength test is conducted on all the nine samples and recorded, as shown in Table 4. Out of nine samples, Sample 3 (S3) and Sample 5 (S5) of SiC and Al_2O_3 reinforced composites have shown the best results. The tensile graphs of S3 are shown in Fig.5. The practical findings matched the theoretical values and found higher tensile strength for the Sample 3 and Sample 5 of the reinforced composites better than the raw Al 6061 material. The joint's shear load is influenced by hard intermetallic compounds and brittleness of the material. The generation of frictional heat increases the tool's rotational speed or decreasing the welding speed, resulting in good enough stirring and mixing of the materials, and hence fine-grains are formed in the nugget zone. A consequent increase in rotational speed improves the formation of intermetallics at the interface of the reinforced region [26]. The significant parameter for this scenario is the rotational speed. If the rotational speed is low, i.e. 900 RPM (S3) and 1150 RPM (S5) for the same composition, then the tensile strength is best. It is evident that if the speed increases, then the distribution of the particles is less and, in turn, resulted in a decrease in tensile strength.

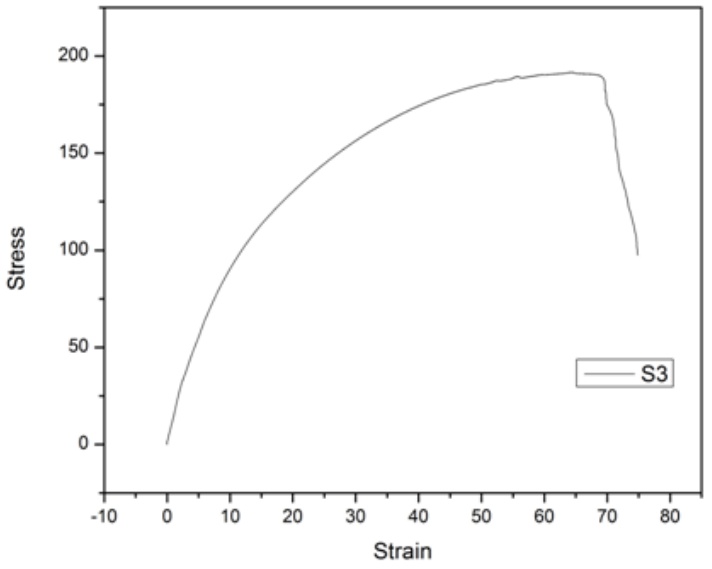

Fig. 5. Tensile strength of SiC and Al_2O_3 for Sample 3 (S3).

Confirmation test:

After the entire experimental evaluation is completed, the optimum setting is identified and observed from the Taguchi analysis. The level of optimum setting is 900 RPM, 15 mm/min travel speed, and composition 3. The confirmation tests for the said optimum setting level had been performed three times. The average ultimate tensile strength of 186 MPa was observed.

Process parameters: Effects on the hardness

There is a necessity to proceed further on the effects of the process parameters on the hardness of the reinforced SiC and Al_2O_3. Fig. 6 is the graph obtained by the results of the microhardness test of the fabricated sample. The hardness values show an increase of hardness from base metal to NZ and HAZ. Out of nine reinforced samples, Sample 3 and Sample 5 have shown better hardness in the NZ. The values are110 and 109 VHN, respectively. As shown in the graph (figure 6), the reinforcement of Al 6061 with SiC and Al_2O_3 had affected the hardness of the material. A remarkable increase in the microhardness of NZ compared to TMAZ and HAZ is noticed. NZ and (Base Material) BM are having more or less the same strength, and those microhardness values were noted. The uniform distribution of SiC and Al_2O_3 particles lead to high microhardness in NZ and HAZ. The rotation speed of the tool and the welding speed predominate the NZ and HAZ width. The width of NZ and HAZ increase with the increasing of tool rotation speed and decrease with the increasing welding speed. The high tool rotation speed created a large heat input and severe plastic flow when a constant welding speed is employed. High welding speed causes low heat input and less plastic flow when the tool's rotation speed is constant. The NZ and HAZ widths are, however, much more influenced by the rotation speed of the tool than by the welding speed [27].

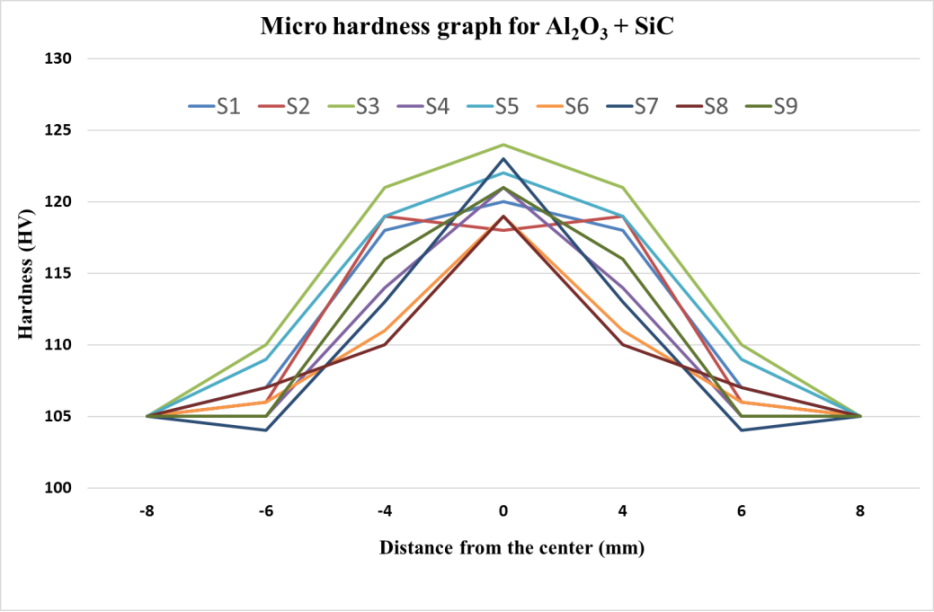

Fig. 6. Hardness profiles of FSP zone.

Microstructure characterization of the sample

Surface texture before FSP was coarse and rough on the Al 6061 processed plates. The same has been depicted in Fig.7, which displays the SEM image. It is found that the samples processed with

(i) 60% of SiC and 40% of Al_2O_3 , RS= 900 RPM, TS= 35 mm/min(S3)

(ii) 60% of SiC and 40% of Al_2O_3, RS=1150 RPM, TS= 25mm/min(S5)

, have reflected better results out of nine samples. The secondary phase particles were found in the range' 0.25 µm – 2 µm'. After FSP, in the nugget zone, the grains are completely recrystallized and formed a smooth and hard surface. The Thermomechanical and Heat affected zones are having irregular and randomly developed grains.

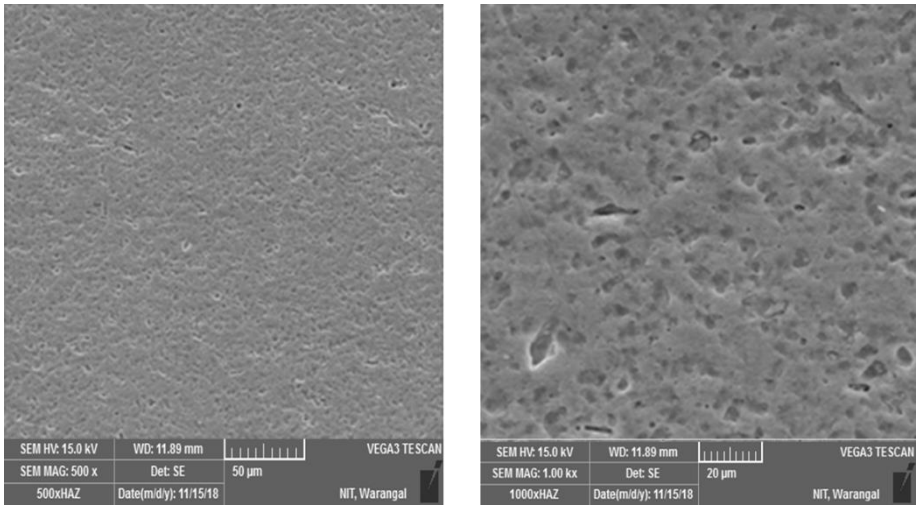

Fig. 7. Al 6061 surface image as-received condition.

Figure 8 (i)-(iii) depicts the SEM images of the FSP processed surface of sample S3. It is observed from the SEM analysis that the processed surface has spherical grains enforced on the aluminum surface. The heat produced by the tool rotation ideally reaches about 0.8 of the melting temperature. This leads to increased redistribution and refining, recrystallization, and production of grains. Aluminum composites with reinforcement of have clustered and distributed heterogeneous microstructure in the matrix [28].

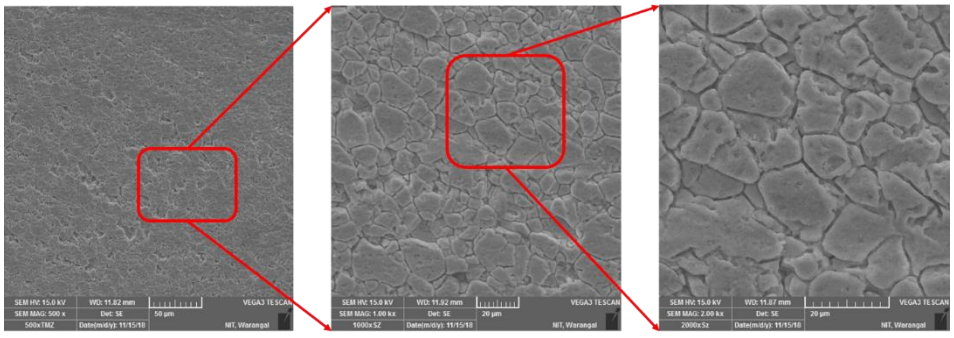

Fig.8. Scanning Electron Microscope images of the processed surface of sample S3.

The presence of different elements can be inspected through EDAX or EDS. The elemental composition and compounds of FSP composite can be identified with the help of EDS-spot- analysis on the fabricated layer. Fig.9 shows the presence of Aluminum, Silicon, Chromium, Copper, and Magnesium. The spectrum discharges the highest elemental presence to peaks.

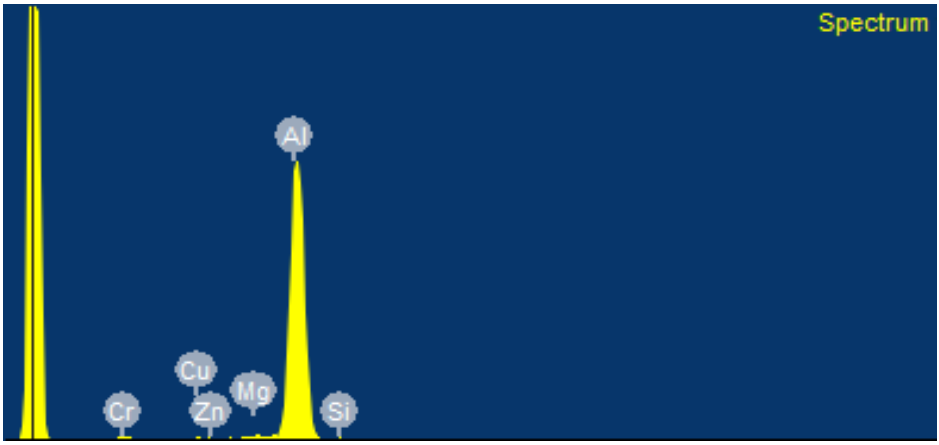

Fig. 9. EDS image of the friction stir processed with 60/40 Weight/volume % SiC/Al_2O_3, at the rotational speed of 900 RPM and travel speed of 35 mm/min (S3).

The comparison in the phases of Al 6061 alloy and reinforced Al 6061 is shown in Fig.10.

This is called the phase identification diagram. The XRD pattern of the SiC and Al_2O_3 reinforced composite shown high intensity when compared to Al 6061 alloy. It is evident from the XRD pattern that the reinforcement of SiC and Al_2O_3 formed the phases after FSP, as expected.

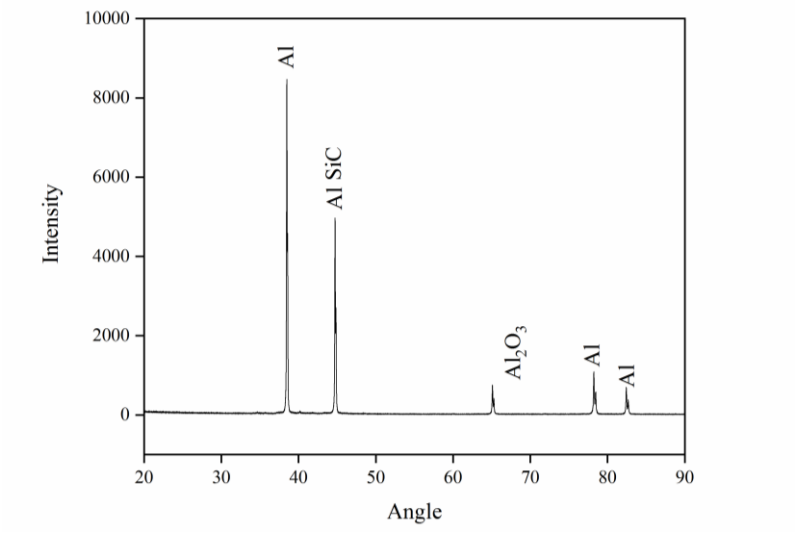

Fig. 10. XRD pattern for sample S3.

Fractography (study after tensile test):

The sample S3, which has shown higher tensile strength, is considered for fractography. Fig.11 elaborates on the fracture behavior of the Al 6061, SiC, and Al_2O_3fabricated product. Only a few SiC and Al_2O_3 particles adhere to the matrix and supporting the tensile behavior of the composite. From the fractography, it is observed that the surface textures are elongated towards the pulling direction i.e. load direction. Hence, from the tensile test and fractography analysis, the fracture behavior of the sample has ductile behavior.

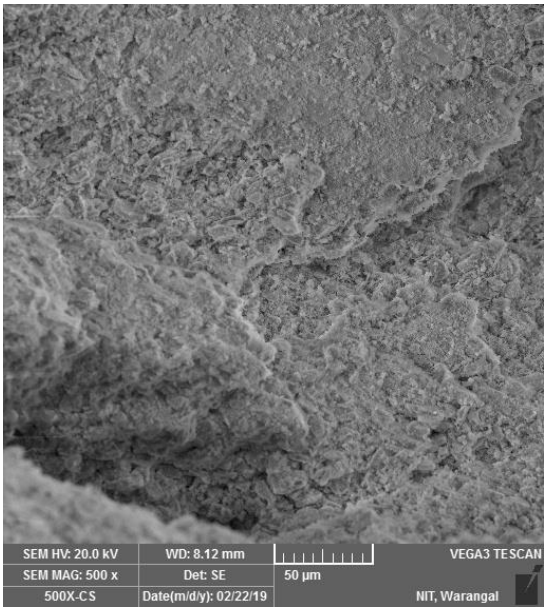

Fig. 11. The fracture surface of composite sample S3.

Conclusions

The effects of process parameters on the fabricated material with the combination of Al 6061 + SiC + Al_2O_3 is the major focus of the work. The surface composite had evident effects on mechanical and microstructure properties on the reinforced composite prepared by FSP. The conclusions drawn depending on the results are:

- The significant change was observed in the mechanical strength of fabricated Al 6061 due to the parameters rotational speed (RS) and travel speed (TS).
- RS of 900 RPM and TS of 15mm/min, for composition3, resulted in maximum tensile strength for the reinforced sample.
- Rotational speed and composition have more influence on the performance of the processed samples than travel speed.
- Fully dense spherical grains are observed on the fabricated samples. From the fractography analysis, the fracture behavior observed is ductile.
- The reinforced sample exhibited high hardness at NZ than in other zones. The increase in the volume of SiC had a positive impact by exhibiting higher microhardness values in the nugget zone.

- While inspecting the microstructure of the Al 6061 composite, the range of '0.25µm - 2µm' secondary phase particles are visible.
- XRD pattern shows that the SiC and Al_2O_3 particles are distributed evenly along the grain boundaries.

References

[1] H. Bakes, D. Benjamin, C.W. Kirkpatrick: Metals handbook, vol. 2. Metals Park, OH: ASM, 1979, 3-23.
[2] Y. Wan, Q. Xue: Tribology letters, 2 (1996) 37-45.
[3] M. Smagorinski, P. Tsantrizos, S. Grenier, M. Entezarian, F. Ajersch: JOM, 48 (1996) 56-59.
[4] T. W. Clyne, P. J. Withers: Cambridge university press, 1995.
[5] E. Rabinowicz, R. I. Tanner, Friction and wear of materials, 1966.
[6] K. G. Budinski: Prentice-Hall, Inc, Englewood Cliffs, New Jersey 07632, United States, 1988. 420.
[7] A. Shafiei-Zarghani, S. F. Kashani-Bozorg, A. Zarei-Hanzaki: Materials Science and Engineering: A, 500 (2009) 84-91.
[8] D. Yadav, R. Bauri: Mater Sci Eng A, 528 (2011) 1326–1333.
[9] H. S. Arora, H. Singh, B. K. Dhindaw: The International Journal of Advanced Manufacturing Technology, 61 (2012) 1043-1055.
[10] A. Azimi, A. Shokuhfar, O. Nejadseyfi: Materials & Design, (1980-2015), 66, (2015) 137-141.
[11] W. B. Lee, Y. M. Yeon, S. B. Jung: Materials transactions, 45 (2004) 1700-1705.
[12] K. Elangovan, V. Balasubramanian: Materials Science and Engineering: A, 459 (2007) 7-18.
[13] R. Palanivel, P. K. Mathews, N. Murugan, I. Dinaharan: Materials & Design, 40 (2012) 7-16.
[14] M. Koilraj, V. Sundareswaran, S. Vijayan, S. K. Rao: Materials & Design, 42 (2012) 1-7.
[15] A. K. Lakshminarayanan, V. Balasubramanian: Transactions of Nonferrous Metals Society of China, 18 (2008) 548-554.
[16] W. Wang, Q. Y. Shi, P. Liu, H. K. Li, T. Li: Journal of materials processing technology, 209 (2009) 2099-2103.
[17] P. Cavaliere: Composites part A: applied science and manufacturing, 36 (2005) 1657-1665.
[18] A. K. Lakshminarayanan, V. Balasubramanian, K. Elangovan,: The International Journal of Advanced Manufacturing Technology, 40 (2009) 286-296.
[19] K. Elangovan, V. Balasubramanian, S. Babu: Materials & Design, 30 (2009) 188-193.
[20] C. M. Rao, K. M. Rao: Materials today: proceedings, 5 (2018) 268-275.
[21] F. Nascimento, T. Santos, P. Vilaça, R. M. Miranda, L. Quintino: Materials Science and Engineering: A, 506 (2009) 16-22.
[22] Z. Y. Ma, R. S. Mishra: Acta materialia, 51 (2003) 3551-3569.
[23] C. M. Rao, K. M. Rao,:International Journal of Engineering & Technology(IJET), 9 (2017) 18-23.

[24] S. Soleymani, A. Abdollah-Zadeh, S. A. Alidokht: Wear, 278 (2012) 41-47.
[25] Y. Cui, L. Wang, J. Ren: Chinese Journal of Aeronautics, 21 (2008) 578-584.
[26] M.H. Shojaeefard, A. Khalkhali, M. Akbari, M. Tahani: Materials & Design, (1980-2015) 52, (2013) 587-592.
[27] L. Dongxiao, Y. Xinqi, C. Lei, H. Fangzhou, S. Hao: Materials & Design, 64 (2014) 251-260.
[28] S. Salih Omar, O. Hengan, W. Sun, D.G. McCartney: Materials & Design, 86 (2015) 61-71.